American Mineralogist, Volume 89, pages 1433–1437, 2004

Mg/Si ratios of aqueous fluids coexisting with forsterite and enstatite based on the phase relations in the Mg_2SiO_4-SiO_2-H_2O system

TATSUHIKO KAWAMOTO,[1,*] KYOKO N. MATSUKAGE,[2] KENJI MIBE,[3] MAIKO ISSHIKI,[4] KOSHI NISHIMURA,[1] NAOKI ISHIMATSU,[5] AND SHIGEAKI ONO[6]

[1]Institute for Geothermal Sciences, Graduate School of Science, Kyoto University, Beppu 874-0903, Japan.
[2]Department of Environmental Sciences, Faculty of Science, Ibaraki University, Mito 310-8512, Japan
[3]Geophysical Laboratory, Carnegie Institution of Washington, 5251 Broad Branch Road, NW, Washington, D.C. 20015, U.S.A.
[4]Japan Synchrotron Radiation Research Institute, SPring-8, Mikazuki, Hyogo 679-5198, Japan
[5]Department of Physical Science, Graduate School of Science, Hiroshima University, Higashi-Hiroshima 739-8526, Japan
[6]Institute for Frontier Research on Earth Evolution, Japan Agency for Marine-Earth Science and Technology, Natsushima, Yokosuka 237-0061, Japan

ABSTRACT

Direct observation of aqueous fluids coexisting with $MgSiO_3$ (enstatite) and/or Mg_2SiO_4 (forsterite) was performed at 0.5–5.8 GPa and 800–1000 °C with an externally heated diamond-anvil cell and synchrotron X-rays. At 1000 °C in the $MgSiO_3$–H_2O system, forsterite crystallizes below 3 GPa but not above that pressure. At 1000 °C in the Mg_2SiO_4–H_2O system, forsterite congruently dissolves into the aqueous fluids up to 5 GPa. These observations suggest that the aqueous fluids coexisting with enstatite and forsterite have Mg/Si < 1 below 3 GPa and 1 < Mg/Si < 2 above that pressure.

Comparison with the previous studies reporting Mg/Si ratios of the aqueous fluid coexisting with enstatite and forsterite indicates that the Mg/Si ratios change rapidly from SiO_2-rich to MgO-rich at around 3 GPa and 1000 °C. This change can be related to possible structural changes of liquid water under these conditions. The aqueous fluids coexisting with enstatite and forsterite do have Mg/Si ratios similar to those found in the partial melts of H_2O-saturated peridotite. Somewhere within the upper mantle, these two fluids unite to form a single regime and cannot be distinguished from each other.

INTRODUCTION

It is known that aqueous fluids can dissolve significant amounts of silicate components under high pressure and temperature conditions. Such fluids can act, therefore, as transfer agents during metamorphism, magmatism, and volcanism (Anderson and Burnham 1965; Nakamura and Kushiro 1974; Manning 1994). Therefore, knowledge of the chemical compositions of silicates dissolved in aqueous fluids is essential to an understanding of the chemical evolution of the Earth's interior.

Since the pioneering work of Nakamura and Kushiro (1974), the chemical compositions of silicates dissolved in aqueous fluids have been characterized by an SiO_2-rich component at relatively shallow depths corresponding to pressures between 1 and 3 GPa (Ryabchikov et al. 1982; Zhang and Frantz 2000). In contrast, recent experimental data above 3 GPa suggested that aqueous fluids coexisting with enstatite ($MgSiO_3$) and forsterite (Mg_2SiO_4) exhibit higher Mg/Si ratios as the pressure increases from 3 GPa up to 10 GPa (Mibe et al. 2002; Stalder et al. 2001). At 3 GPa and 1100 °C, the Mg/Si ratios within the aqueous fluids varies from 0.1 Mg/Si (Ryabchikov et al. 1982) to 1.2 Mg/Si (Mibe et al. 2002).

In previous research on this subject, experimental products quenched from high temperature and pressure conditions were examined. In such cases, there is always the question of whether an observed phase was actually formed under the elevated pressure and temperature conditions or whether it may have crystallized during the temperature quench. In the present study, we aim to avoid this problem by in-situ observation using synchrotron X-rays and an externally heated diamond-anvil cell to cover a pressure range from 0.5 GPa to 5 GPa. Although there are some limitations to the detection of small amounts of phases by collimated X-rays in the present experimental technique, in-situ X-ray observation without a temperature gradient (Bassett et al. 1993) can shed light on the phase relations including aqueous fluids. On a basis of the chemographic relations in the Mg_2SiO_4-SiO_2-H_2O system, we report the pressure and temperature conditions where the Mg/Si ratio of the aqueous fluids coexisting enstatite and forsterite becomes equal to the unity.

EXPERIMENTAL METHODS

High-pressure and high-temperature experiments were carried out with externally heated Bassett-type diamond-anvil cells set to a 60° open angle (Bassett et al. 1993; Shen and Keppler 1995; Bureau and Keppler 1999; Zotov and Keppler 2000). An enstatite glass chip was loaded into the diamond-anvil cell together with a piece of gold foil and some distilled water. A limited number of experiments were conducted with synthetic proto-enstatite crystals and with forsterite crystals instead of enstatite glasses (Table 1). The externally heated Bassett-type diamond-anvil cell was pressurized within a worm gear box as follows: the upper platen of the cell was fixed on the roof of the box, the lower platen was forced to move upward, three stop pins were set to maintain the distance between two platens and finally three cramp pins were adjusted by a torque driver to maintain a constant pressure. Such a worm gear box was originally designed by Dr. K. Takemura of National Institute for Materials Science, Tsukuba, Japan, for his diamond-anvil

* E-mail: kawamoto@bep.vgs.kyoto-u.ac.jp

cell (Takemura et al. 1979). Rhenium gaskets with an initial thickness of 0.25 mm were pre-indented between diamond anvils of 0.6 or 1 mm culet size. A 0.2 or 0.4 μm hole was electrically eroded in the gasket to serve as a sample container. The sample was heated by controlling DC power supplies to coils made from 0.3 mm diameter molybdenum or 87%Pt-13%Rh wire, wrapped around WC or Si_3N_4 seats supporting the diamond anvils. Temperature at the sample location and under ambient pressure was measured with two K-type thermocouples attached to each diamond. Rigorous temperature control, which maintains the temperature of each diamond within a few °C, is one advantage of using the Bassett-type of externally heated diamond-anvil cell, and eliminates possible problems associated with phase separations along temperature gradients. The temperature was calibrated by visual observation of the melting points of $NaNO_3$ (307 °C), CsCl (645°C), and NaCl (801 °C) at ambient pressure.

At high temperature, the cell was flushed with 98% argon-2% hydrogen gas to prevent oxidation of the diamonds and the metal constituents. The maximum temperatures in the present experiments were limited to about 1000 °C mainly due to the necessity to avoid graphitization of the diamonds over the 20–30 minute observation period. Even so, after the experiment, the support surfaces of the diamond anvils were found to be less transparent due to the deposition of Co and Ni binder materials from WC seats or stainless steel constituents of the cell. In addition, some graphitization and oxidation of the diamonds took place. The culet surfaces of the diamonds were chemically stable, although many diamonds were cracked during heating.

Angle-dispersive X-ray diffraction (XRD) experiments were performed using the diamond-anvil cell at synchrotron beam line BL04B2 in SPring-8 synchrotron facility operating at 8 GeV and 100 mA in Nishi-Harima, Japan (Isshiki et al. 2001). Use of this synchrotron X-ray system enables the mineral coexisting with the aqueous fluids under high pressure and temperature conditions to be identified. The incident X-ray beam was monochromatized to a wavelength of 0.328 Å and its cross-section was collimated to 0.04×0.04 μm^2 or a 0.1 μm diameter circle. Angle-dispersive XRD patterns were obtained with an imaging plate placed at about 450 mm from the sample and using an acquisition time of 3–5 minutes. CeO_2 was used as a standard source of known wavelength. The recorded intensities on the imaging plates were integrated as a function of 2 theta to produce conventional one-dimensional diffraction profiles. Pressure was determined from the measured unit-cell volume of gold foils using the *P-V-T* equation of state for gold given by Anderson et al. (1989) from four diffraction lines (111, 200, 220, 311) at elevated temperature. The error for the pressure was estimated from the standard deviation of the calculated pressure from the above-mentioned four lines of gold. The precision was better than 0.3 GPa.

Portions of quenched crystals with grain sizes in the range 0.005–0.02 μm diameter were recovered, embedded in epoxy together with a gasket, and then polished. In order to identify crystalline phases, unpolarized Raman spectra of the unpolished and polished samples were measured with a Raman microscope with a 532 nm YAG laser for sample excitation, holographic transmission gratings, and a CCD Raman shift detector working in the 100–4500 cm^{-1} range (Kaiser HoloLab 5000 system). A transmission grating yields higher light throughput than conventional reflection gratings. Quenched phases also were examined with a scanning electron microscope (JEOL 5310) and their chemical compositions were determined with an energy dispersive system (Oxford LINK-2). X-ray mapping of some quenched run products was conducted with a wavelength-dispersive electron microprobe analyzer (JEOL Superprobe 8900) at the Department of Earth and Planetary Sciences, Tokyo Institute of Technology.

TABLE 1. Summary of experimental conditions and phases

Starting material	Run no.	Temperature(°C)	Pressure (GPa)	Phases
En crystal +H_2O	m1-013	900	1.7	Au, En, Fo
	m1-015	900	0.9	Au, En, Fo
	m1-016	1000	1.0	Au, En, Fo*
En glass + H_2O	m2-006	1000	0.5	Au, En, Fo*
	k1003	1000	0.6	Au, En, Fo
	k1-004	800	1.0	Au, En, Fo
	k1-005	800	1.0	Au, En, Fo
	k1-006	900	1.0	Au, En, Fo
	b1-009	1000	1.2	Au, En, Fo*
	m1003	1000	1.5	Au, En, Fo
	b1006	1000	2.6	Au, En, Fo*
	k2-003	1000	2.7	Au, En, Fo*
	b2-003	800	3.6	Au, En
	b2-004	900	4.5	Au, En
	b2-005	1000	5.2	Au, En
	t007	1000	3.9	Au, En
	3b1-003	800	2.8	Au, En
	3b1-004	800	3.1	Au, En
	3b1-005	800	3.5	Au, En
	3b1-006	800	4.1	Au, En
	3b1-007	900	4.8	Au, En
	3b1-008	900	5.8	Au, En
	3m2-004	900	4.0	Au, En
	3m2-005	900	4.5	Au, En
	3m2-006	900	4.8	Au, En
	3m2-007	900	4.6	Au, En
	3m2-008	900	5.8	Au, En
Fo crystal + H_2O	m3-003	805	2.1	Au, Fo
	m3-005	900	1.5	Au, Fo
	m3-006	1000	1.3	Au, Fo
	b3-003	900	3.6	Au, Fo
	b3-004	1000	3.2	Au, Fo
	b1-007	1000	5.0	Au, Fo

Notes: En = enstatite; Fo = forsterite; Fo* = forsterite observed in quench sample.

EXPERIMENTAL RESULTS

A typical XRD pattern is reproduced in Figure 1. In the present experiments, all $MgSiO_3$ crystals were found to be clinoenstatite, although orthoenstatite is stable under the present pressure and temperature conditions on the basis of a previous experimental study (Ulmer and Stalder 2001). This disparity suggests that the observed clinoenstatite may have been formed under disequilibrium conditions. However, because chemical compositions of those polymorphs are identical, the exact nature of the enstatite polymorph may not affect the Mg/Si ratios of the aqueous fluids.

In experimental charges where forsterite was detected by XRD at high pressure and temperature, the presence of forsterite was confirmed by micro-Raman spectroscopy and its chemical composition was determined by electron microprobe analysis (Table 1). In some experiments, a few large forsterite crystals (0.01–0.02 μm in diameter) were observed in the quenched run products, although only enstatite was detected by in situ XRD at high pressure and temperature. In those experiments, only a few percent forsterite was observed. Such low concentrations are less than the detection limit of the X-ray method in which a

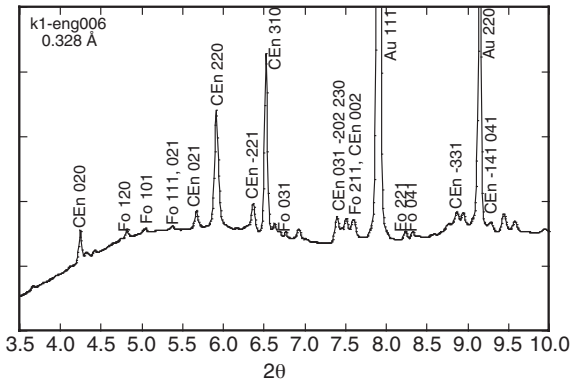

FIGURE 1. X-ray diffraction pattern obtained using the angle-dispersive technique with the diamond-anvil cell experiments at 900 °C and 1 GPa. Mg_2SiO_4 forsterite crystallizes in the $MgSiO_3$-H_2O system suggesting that Mg/Si ratio of the aqueous fluid is less than unity. Peak identifications are as follows: Cen = $MgSiO_3$ clinoenstatite; Fo = Mg_2SiO_4 forsterite; Au = gold.

0.04 μm collimator was used. It is difficult to avoid the growth of large crystals in the aqueous fluids. The modal proportions of forsterite crystals in an experimental sample depend on the Mg/Si ratio of the aqueous fluid and on the water content of the starting mixture. Values of the Mg/Si ratio in the aqueous fluids of close to unity, coupled with less water in the starting mixture may have resulted in less forsterite in the experimental charge. In the present study, however, the large forsterite crystals are interpreted as representing a stable phase corresponding to the pressure and temperature conditions before quenching, even though it could not be detected by the in-situ X-ray technique.

In the 0.5–2.8 GPa pressure range, forsterite crystallizes at 1000 °C in the $MgSiO_3$-H_2O system (Figs. 1 and 2A, Table 1). The aqueous fluids can therefore dissolve more SiO_2–rich components than MgO-rich components, resulting in an Mg/Si atomic ratio of less than unity (Fig. 2B). In contrast, at pressures greater than 3.9 GPa, enstatite dissolves congruently at 1000 °C, whereas forsterite dissolves congruently up to 5.0 GPa (Table 1). These data suggest that the aqueous fluids coexisting with enstatite and forsterite can have Mg/Si ratios in the range 1<Mg/Si<2 under these conditions (Fig. 2C). In the present experimental configurations, the Mg/Si ratios of the aqueous fluids are fixed by the starting material. As can be seen in Figures 2B and 2C, the fluid compositions can change along the univariant curve. Therefore, the present experiments cannot determine the Mg/Si ratios but only suggest the chemical ranges of the aqueous fluids coexisting with enstatite and forsterite: Mg/Si<1 or 1<Mg/Si<2.

Mg/Si ratios of aqueous fluids as a function of pressure and temperature

In Figure 2A and in the previous studies (Kushiro et al. 1968; Mibe et al. 2002), the Mg/Si = 1 curve shows a positive relation with temperature. The congruent dissolution of enstatite was reported at 1000 °C and 3 GPa, and the incongruent dissolution at 1100 °C and higher temperatures at 3 GPa by Kushiro et al. (1968), Fig. 2A. The Mg/Si ratio of aqueous fluid coexisting with forsterite and enstatite was demonstrated to decrease with increasing temperature at 5 GPa; Mg/Si = 1 can be located at 1200 °C and 5 GPa (Mibe et al., 2002). The Mg/Si = 1 curve can be located at 2.5 GPa and 800 °C (Fig. 2A), although it is constrained by fewer experimental data.

On a basis of phase relations in the Mg_2SiO_4-SiO_2-H_2O system using a piston-cylinder type of high pressure and high temperature apparatus, Zhang and Frantz (2000; 1–2 GPa, 900–1000 °C) and Ryabchikov et al. (1982; 3 GPa, 900–1100 °C) suggested that aqueous fluids are characterized by an SiO_2-rich nature, with Mg/Si ratios increasing slightly with an increase in pressure. An Mg/Si ratio of 1.2 within aqueous fluids at 3 GPa and 1100 °C was reported by Mibe et al. (2002) based on an experiment using a multi-anvil apparatus. This value was supported by a single experiment where forsterite was not observed, although there is the possibility of overlooking trace amounts of forsterite in the experimental charge. The experimental data suggest that the Mg/Si ratios of aqueous fluids can change rapidly from an SiO_2-rich to an MgO-rich regime at around 3 GPa (Fig. 3A), although no single series of experiments detected the drastic change of Mg/Si ratios at around 3 GPa. This is mainly because experiments at around 3 ± 1 GPa are difficult to carry out with either multi-anvil type or piston-cylinder type of high pressure and temperature apparatus.

Liquid H_2O might change its structure under these conditions. Kawamoto et al. (2004) reported the Raman spectra of water

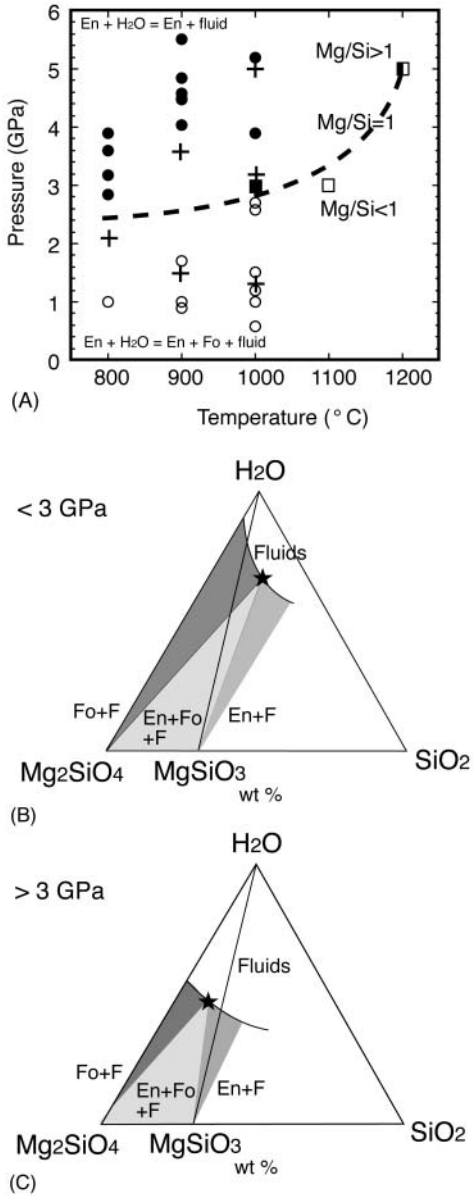

FIGURE 2. (A) Experimental results showing Mg/Si ratios of silicate components in aqueous fluids coexisting with enstatite (En) and forsterite (Fo) based on chemographic analyses. Open circles and square (Kushiro et al. 1968) = En + H_2O = En + Fo + fluid; solid circles and square (Kushiro et al. 1968) = En + H_2O = En + fluid; half solid square = Mg/Si = 1 based on chemical analyses of dendritic portion (Mibe et al. 2002); cross = Fo + H_2O = Fo + fluid. **(B, C)** Schematic isothermal sections of Mg_2SiO_4-SiO_2-H_2O system at 1000 °C. Stars represent possible H_2O fluid coexisting with Fo and En. The H_2O concentrations of the fluids were not determined in the present study but taken after the previous study (Mibe et al. 2002). At pressures lower than 3 GPa, the aqueous fluids (F) coexisting with En and Fo have Mg/Si < 1, and at pressures greater than 3 GPa, they have 1 < Mg/Si < 2.

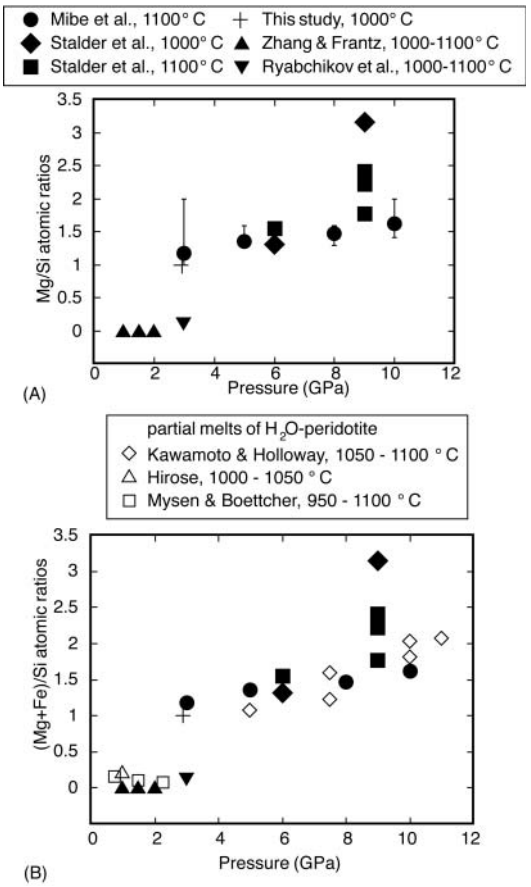

FIGURE 3. (A) Pressure and Mg/Si ratios of aqueous fluids coexisting with forsterite and enstatite at a temperature range from 1000 to 1100 °C (Ryabchikov et al. 1982; Zhang and Frantz 2000; Stalder et al. 2001; Mibe et al. 2002). **(B)** Comparison of aqueous fluid chemistry with partial melt chemistry of H_2O-saturated mantle peridotite (Mysen and Boettcher 1975; Hirose 1997; Kawamoto and Holloway 1997). See text for discussion.

under high-temperature and -pressure conditions and showed a discontinuity in the pressure dependence of the OH-stretching frequency at 0.4 ± 0.1 GPa at 25 °C, 1.0 ± 0.1 GPa at 100 °C and 1.3 ± 0.1 GPa at 300 °C. They suggested a structural change from sparse water to dense water under these conditions. Such structural changes of water should affect on the solution chemistry of aqueous fluids under these conditions.

Quench experiments were conducted in the Mg_2SiO_4-$MgSiO_3$-H_2O system with a Walker-type multi-anvil apparatus at pressures from 6 GPa to 10.5 GPa (Stalder et al. 2001). The chemical compositions of deposits from aqueous fluids trapped in diamond aggregates were analyzed by a laser ablation-induced coupled plasma mass spectrometer (LA-ICP-MS): the measured Mg/Si ratios are 1.5 at 6 GPa and around 2 at 9 GPa in a temperature range between 1000–1100 °C. Based on phase relations in the Mg_2SiO_4-SiO_2-H_2O system using a Kawai-type multi-anvil apparatus, the following Mg/Si ratios were estimated at 1100 °C: 1.2 at 3 GPa, 1.4 at 5 GPa, 1.5 at 8 GPa, and 1.6 at 10 GPa (Fig. 3A, Mibe et al. 2002). These two sets of data are concordant with each other with respect to Mg/Si ratios (Fig. 3A), and suggest that the Mg/Si of aqueous fluids can exceed 2 in the pressure range between 8 GPa (Stalder et al. 2001) and 13 GPa (Mibe et al. 2002). If this is the case, then enstatite should crystallize in the Mg_2SiO_4-H_2O system due to the presence of MgO-rich aqueous fluids. Enstatite was actually found in the Mg_2SiO_4-H_2O system at a pressure range from 7 to 10 GPa, although this enstatite was interpreted as a quench product crystallized from SiO_2-rich fluids (Luth 1995). Congruent dissolution of enstatite and forsterite was reported at 1100 °C, and 5.5 GPa and 7.7 GPa, respectively (Inoue 1994). In the present study, forsterite dissolves congruently in aqueous fluids up to 5 GPa (Table 1). Whether the aqueous fluids become more mafic than olivine is an important question and remains to be determined by in-situ observation.

H_2O-rich melts or silicate-rich aqueous fluids?

The chemical compositions of partial melts of H_2O-saturated peridotite also are characterized by high Mg/Si ratios (Inoue 1994; Irifune et al. 1998; Kawamoto and Holloway 1997). Figure 3B compares the partial melt chemistry of H_2O-saturated mantle peridotite (Mysen and Boettcher 1975; Hirose 1997; Kawamoto and Holloway 1997) with the H_2O fluid data with respect to (Mg+Fe)/Si ratio as a function of pressure. Both datasets show a similar variation and overlap each other. This result might suggest that there is no distinction between H_2O-rich melts and silicate-rich fluids. Alternatively, the partition coefficients of Mg and Si between the partial melts and the aqueous fluids are similar under these conditions.

Previous experiments determined the H_2O-saturated solidus temperature identifying abrupt changes in chemical compositions of the minerals and/or the appearance of dendritic textures with increasing temperature at a given pressure (Inoue 1994; Kawamoto and Holloway 1997; Irifune et al. 1998; Stalder et al. 2001; Mibe et al. 2002). Some previous workers distinguished two types of dendritic texture: one quenched from partial melt and the other from aqueous fluids (Irifune et al. 1998; Litasov and Ohtani 2002). However, they mentioned that it is difficult to distinguish between these types of texture at pressures greater than 10–13 GPa. In addition to this difficulty, none of the experiments demonstrated the coexistence of H_2O-rich silicate melts and silicate-rich aqueous fluids in either the MgO-SiO_2-H_2O system or in a peridotite system under any combination of pressure and temperature. As the critical temperature between aqueous fluids and silicate melts decreases with increasing pressure (Figs. 4A and 4B, Paillat et al. 1992; Shen and Keppler 1997; Bureau and Keppler 1999), it should meet an H_2O-saturated solidus temperature with increasing pressure (Fig. 4C). Both the chemical similarity and experimental observation suggest a continuous change between those two fluids somewhere in the upper mantle. If so, the traditional H_2O-saturated solidus temperature may represent a temperature where the concentration of silicate components dissolved into aqueous fluids increases drastically (Fig. 4C) and may therefore justify its description as a "practical solidus" (Iwamori 1998). The shape of the phase diagram should be investigated as a function of pressure as this may change the present scheme of magma generation in the earth's mantle because all terrestrial magmas can have H_2O (Thompson 1992).

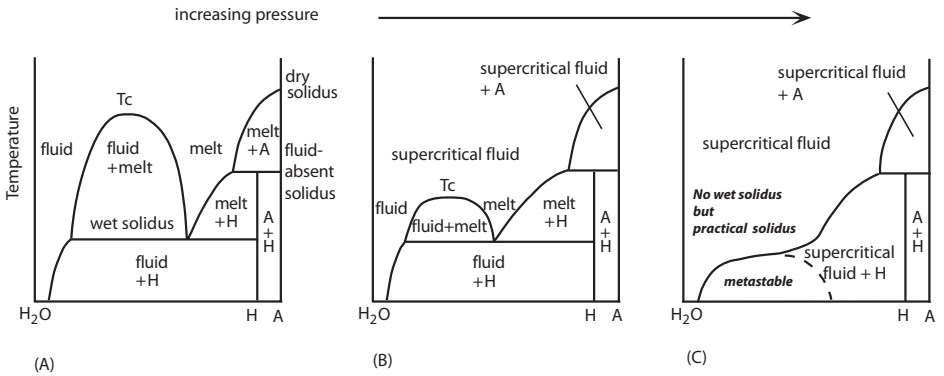

FIGURE 4. Schematic phase diagrams in the system of mineral A and H_2O. H is a hydrous mineral. **(A, B)** As pressure increases, a critical temperature (*T*c) between H_2O-bearing silicate melt and silicate-bearing H_2O fluid decreases. **(C)** The *T*c meets the H_2O-saturated solidus temperature in the system (at a second critical point or critical end point). At pressures beyond that of the second critical point, there is no difference between melts and fluids. In this case there is no H_2O-saturated solidus temperature.

ACKNOWLEDGMENTS

B. Bassett, T. Kondo, N. Zotov, J. Sowerby, H. Keppler, Y. Tatsumi, N. Funamori, and E. Takahashi are appreciated for their assistance and valuable suggestions. Forsterite crystals were synthesized by K. Ito. Comments on an earlier version of the manuscript by B. Mysen, N. Zotov, H. Keppler, H. Iwamori, and J. Matthews improved the manuscript. Careful reviews by B. Mysen and B. Bassett clarified the manuscript. This work was supported by JASRI/SPring-8, the Nissan Science Foundation, the Reimei Research of JAERI, Kyoto University, the Japanese Society for the Promotion of Sciences, the Ministry of Education, Culture, Sports, Science and Technology and Grant-in-Aid for the 21st Century COE Program.

REFERENCES CITED

Anderson, G.M. and Burnham, C.W. (1965) The solubility of quartz in supercritical water. American Journal of Science, 263, 494–511.

Anderson, O.L., Isaak, D.G., and Yamamoto, S. (1989) Anharmonicity and the equation of state for gold. Journal of Applied Physics, 65, 1534–1543.

Bassett, W.A., Shen, A.H., Bucknum, M., and Chou, I.-M. (1993) A new diamond anvil cell for hydrothermal studies to 2.5 GPa and –190 °C to 1200 °C. Review of Scientific Instruments, 64, 2340–2345.

Bureau, H. and Keppler, H. (1999) Complete miscibility between silicate melts and hydrous fluids in the upper mantle; experimental evidence and geochemical implications. Earth and Planetary Science Letters, 165, 187–196.

Inoue, T. (1994) Effect of water on melting phase relations and melt composition in the system Mg_2SiO_4-$MgSiO_3$-H_2O up to 15 GPa. Physics of the Earth and Planetary Interiors, 85, 237–263.

Irifune, T., Kubo, N., Isshiki, M., and Yamasaki, Y. (1998) Phase transformations in serpentine and transportation of water into the lower mantle. Geophysical Research Letters, 25, 203–206.

Isshiki, M., Ohishi, Y., Goto, S., Takeshita, K., and Ishikawa, T. (2001) High-energy X-ray diffraction beamline:BL04B2 at SPring-8. Nuclear Instruments and Methods in Physics Research Section A, 467–8, 663–666.

Iwamori, H. (1998) Transportation of H_2O and melting in subduction zones. Earth and Planetary Science Letters, 160, 65–80.

Hirose, K. (1997) Melting experiments on lherzolite KLB-1 under hydrous conditions and generation of high-magnesian andesitic melts. Geology, 25, 42–44.

Kawamoto, T. and Holloway, J.R. (1997) Melting temperature and partial melt chemistry of H_2O-saturated mantle peridotite to 11 gigapascal. Science, 276, 240–243.

Kawamoto, T., Ochiai, S., and Kagi, H. (2004) Changes in the structure of water deduced from the pressure dependence of the Raman OH frequency. Journal of Chemical Physics, 120, 5867–5870.

Kushiro, I., Yoder, H.S.J., and Nishikawa, M. (1968) Effect of water on the melting of enstatite. Geological Society of America Bulletin, 79, 1685–1692.

Litasov, K. and Ohtani, E. (2002) Phase relations and melt compositions in CMAS-pyrolite-H_2O system up to 25 GPa. Physics of the Earth and Planetary Interiors, 134, 105–127.

Luth, R.W. (1995) Is phase A relevant of the Earth's mantle? Geochimica et Cosmochimica Acta, 59, 679–682.

Manning, C.E. (1994) The solubility of quartz in the lower crust and upper mantle. Geochimica et Cosmochimica Acta, 58, 4831–4839.

Mibe, K., Fujii, T., and Yasuda, A. (2002) Composition of aqueous fluid coexisting with mantle minerals at high pressure and its bearing on the differentiation of the Earth's mantle. Geochimica et Cosmochimica Acta, 66, 2273–2285.

Mysen, B.O. and Boettcher, A.L. (1975) Melting of a hydrous mantle: II. Geochemistry of crystals and liquids formed by anatexis of mantle peridotite at high pressures and temperatures as a function of controlled activities of water, hydrogen, and carbon dioxide. Journal of Petrology, 16, 549–593.

Nakamura, Y. and Kushiro, I. (1974) Composition of the gas phase in Mg_2SiO_4-SiO_2-H_2O at 15 kbar. Carnegie Institution of Washington Year Book, 73, 255–258.

Paillat, O., Elphick, S.C., and Brown, W.L. (1992) Solubility of water in $NaAlSi_3O_8$ melts: a re-examination of Ab- H_2O phase relationships and critical behavior at high pressures. Contributions to Mineralogy and Petrology, 112, 490–500.

Ryabchikov, I.D., Schreyer, W., and Abraham, K. (1982) Compositions of aqueous fluid in equilibrium with pyroxenes and olivines at mantle pressures and temperatures. Contributions to Mineralogy and Petrology, 79, 80–84.

Shen, A.H. and Keppler, H. (1995) Infrared spectroscopy of hydrous silicate melts to 1000 degrees C and 10 kbar; direct observation of H_2O speciation in a diamond-anvil cell. American Mineralogist, 80, 1335–1338.

——— (1997) Direct observation of complete miscibility in the albite-H_2O system. Nature, 385, 710–712.

Stalder, R., Ulmer, P., Thompson, A.B., and Günther, D. (2001) High pressure fluids in the system MgO-SiO_2-H_2O under upper mantle conditions. Contributions to Mineralogy and Petrology, 140, 607–618.

Takemura, K., Shimomura, O., Tsuji, K., and Minomura, S. (1979) Diamond-anvil pressure cell for x-ray diffraction with SSD and PSPC system. High Temperatures-High Pressures, 11, 311–316.

Thompson, A.B. (1992) Water in the Earth's upper mantle. Nature, 358, 295–302.

Ulmer, P. and Stalder, R. (2001) The $Mg(Fe)SiO_3$ orthoenstatite-clinoenstatite transitions at high pressures and temperatures determined by Raman-spectroscopy on quenched samples. American Mineralogist, 86, 1267–1274.

Zhang, Y.-G. and Frantz, J.D. (2000) Enstatite-forsterite-water equilibria at elevated temperatures and pressures. American Mineralogist, 85, 918–925.

Zotov, N. and Keppler, H. (2000) In-situ Raman spectra of dissolved silica species in aqueous fluids to 900 °C and 14 kbar. American Mineralogist, 85, 600–604.

MANUSCRIPT RECEIVED JULY 17, 2003
MANUSCRIPT ACCEPTED MARCH 23, 2004
MANUSCRIPT HANDLED BY YINGWEI FEI